

Signomial Programming Models for Aircraft Design

Philippe G. Kirschen,^{*} Edward E. Burnell,[†] and Warren W. Hoburg[‡]
Massachusetts Institute of Technology, Cambridge, Massachusetts, 02139, USA

Due to the coupled nature of aircraft system design, it is important to consider all of the major subsystems when trying to optimize a configuration. This, however, is easier said than done, particularly because each individual subsystem model can be arbitrarily complex, thus making optimization difficult. By restricting an optimization problem to have a certain mathematical structure, significantly more effective and tractable solution techniques can be used. Geometric programming, an example of one such technique, guarantees finding a globally optimal solution. Although it has been shown that geometric programming can be used to solve some conceptual aircraft design problems, the required formulation can prove too restrictive for certain relationships. Signomial programming is a closely related relaxation of geometric programming that offers enhanced expressiveness, but without the guarantee of global optimality. Despite this, solution methods for signomial programs are disciplined and effective. In the present work, signomial programming models are proposed for optimal preliminary sizing of the vertical tail, fuselage, and landing gear of a commercial aircraft with a tube-and-wing configuration. Signomial programming's relaxed formulation allows it to handle some of the key constraints in tail, fuselage, and landing gear design and therefore a significant improvement in fidelity over geometric programming models is achieved. The models are readily extensible and easily combined with other models, making them effective building blocks for a full aircraft model. A primary contribution of this work is to demonstrate signomial programming as a viable tool for multidisciplinary aircraft design optimization.

I. Introduction

Geometric Programming (GP)^a is an optimization technique that combines the expressiveness of non-linear objectives and constraints with the mathematical rigor of convexity to provide a unique and powerful approach to the problem of multidisciplinary aircraft design optimization. For problems that can be formulated as **Geometric Programs (GPs)**, modern solvers guarantee *globally* optimal solutions, are extremely fast, and return local sensitivities at no extra cost, thanks to the principle of lagrange duality. In previous work, Hoburg [1] shows, firstly, that many models common to aircraft design can be represented directly in **GP-compatible** form, and, secondly, that there are a number of innovative ways of dealing with models that cannot, including, but not limited to, changes of variables and **GP-compatible** fitting methods. Finally, it is also shown that such problems can be solved efficiently using a standard laptop computer. The aircraft design problem solved in [1] includes models for steady level flight, range, takeoff distance, landing speed, sprint flight condition, actuator disk propulsive efficiency, simple drag and weight buildups, and beam wing box structure.

Due to these promising initial results, there is a strong desire to extend the use of **GP** for aircraft design both in breadth, by considering more aspects of the aircraft design problem, and in depth, by increasing the fidelity of the models used. Unfortunately, the restrictions on the formulation of **GPs** mean that not all aircraft design constraints can be readily implemented as part of a **GP**. A generalization of **GP** called **Signomial Programming (SP)**, helps to address this by allowing constraints with less restrictive formulations [2]. A relatively small relaxation in the restriction on problem formulation means that **SP** can handle a significantly more general set of problems than **GP**, but this comes at an equally significant cost: **SP** does not boast the same guarantee of global optimality as **GP**. Despite this, solution methods remain disciplined and effective by leveraging the *difference of convex program* structure of **SP**.

Signomial programming is important for aircraft design for two reasons: it allows a modeler to leverage some of the powers of **GP** on models that are not **GP-compatible**, and it enables increasing fidelity where it is not possible to do so in a **GP-compatible** way. From the authors' limited experience, only a small proportion of the constraints in aircraft design models require signomials, if any. In many cases, however, omitting these constraints would mean failing to capture an important design consideration and would therefore be too crude. Sometimes, the constraint in question is

^{*}Graduate Student, Department of Aeronautics and Astronautics, MIT

[†]Graduate Student, Department of Mechanical Engineering, MIT

[‡]Assistant Professor, Department of Aeronautics and Astronautics, MIT

^aThe "GP" acronym is overloaded, referring both to geometric programs - the class of optimization problem discussed in this work - and geometric programming - the practice of using such programs to model and solve optimization problems. The same is true of the "SP" acronym.

the only constraint that keeps one or more design variables meaningfully bounded. Thus, a sacrifice of optimization quality and robustness is made in exchange for obtaining dual feasibility and/or higher model fidelity. It is important to stress that the purpose of this work is not to use **SP** liberally, but rather to use it in a targeted and precise manner, where the marginal cost of introducing a signomial constraint can be justified by an adequate increase in model fidelity or accuracy. Because they result in convex restrictions on the feasible set, monomial and posynomial constraints are still viewed as the preferred approach, wherever possible.

The purpose of this work is to develop **SP** models for design of the vertical tail, fuselage, and landing gear of a commercial aircraft. More specifically, these models determine optimal values for the preliminary geometry, positioning and weight of each subsystem. The models created are readily extensible - constraints can be added and made more sophisticated at little cost - and are also easily combined with each other to capture the strong coupling between the subsystems. The ultimate goal of this line of work is to develop a full aircraft model that considers every major subsystem as well as economic and operational factors. The present work is an intermediate step in achieving this goal. To the authors' best knowledge, this is the first published work on **SP** applied to aircraft design.

There has been extensive research in **Multidisciplinary Design Optimization (MDO)** methods for conceptual aircraft design [3–7]. Of the many different frameworks in the literature, **TASOPT** [5] is particularly relevant to the present work because of its use of physics based models, medium fidelity analytical models, and multidisciplinary considerations of aircraft subsystems. Some common challenges faced in multidisciplinary design optimization include models that are too computationally expensive to be practical for a designer; final results that are sensitive to the choice of baseline design; evaluations of black box functions, about which an optimizer knows very little; and coupling of different analysis tools that requires delicate wiring between models, and generally another layer of complexity and opacity.

II. Background

To motivate the value of signomial programming, we begin by introducing the topic of geometric programming, and briefly discussing its strengths and limitations. We then discuss the relaxation from a geometric program to a signomial program and its effect on modeling expressiveness and on finding an optimal solution. Finally, we define some of the terminology used in this work.

A. Geometric Programming

First introduced in 1967 by Duffin, Peterson, and Zener [8], a geometric program is a specific type of constrained, nonlinear optimization problem that becomes convex after a logarithmic change of variables. Modern **GP** solvers employ primal-dual interior point methods [9] and are extremely fast. A typical sparse **GP** with tens of thousands of decision variables and one million constraints can be solved on a desktop computer in minutes [2]. Furthermore, these solvers do not require an initial guess and guarantee convergence to a *global* optimum, whenever a feasible solution exists. Being able to find optimal solutions without needing an initial guess makes the technique particularly useful for conceptual aircraft design, where it is important that results are not biased by preconceptions of what an optimal aircraft should look like.

These impressive properties are possible because **GPs** represent a restricted subset of nonlinear optimization problems. In particular, the objective and constraints can only be composed of *monomial* and *posynomial* functions.

A *monomial* is a function of the form

$$m(\mathbf{u}) = c \prod_{j=1}^n u_j^{a_j}, \quad (1)$$

where $a_j \in \mathbb{R}$, $c \in \mathbb{R}_{++}$, and $u_j \in \mathbb{R}_{++}$. For instance, the familiar expression for lift, $\frac{1}{2}\rho V^2 C_L S$, is a monomial with $\mathbf{u} = (\rho, V, C_L, S)$, $c = 1/2$, and $\mathbf{a} = (1, 2, 1, 1)$.

A *posynomial* is a function of the form

$$p(\mathbf{u}) = \sum_{k=1}^K c_k \prod_{j=1}^n u_j^{a_{jk}}, \quad (2)$$

where $\mathbf{a}_k \in \mathbb{R}^n$, $c_k \in \mathbb{R}_{++}$, and $u_j \in \mathbb{R}_{++}$. Thus, a posynomial is simply a sum of monomial terms, and all monomials are also posynomials (with just one term).

In plain English, a **GP** minimizes a posynomial objective function, subject to monomial equality constraints and posynomial inequality constraints. The standard form of a geometric program in mathematical notation is as follows:

$$\begin{aligned}
& \text{minimize} && p_0(\mathbf{u}) \\
& \text{subject to} && p_i(\mathbf{u}) \leq 1, \quad i = 1, \dots, n_p, \\
& && m_i(\mathbf{u}) = 1, \quad i = 1, \dots, n_m,
\end{aligned} \tag{3}$$

where the p_i are posynomial (or monomial) functions, the m_i are monomial functions, and $\mathbf{u} \in \mathbb{R}_{++}^n$ are the *decision variables*.

Although this form may appear restrictive, surprisingly many physical constraints and objectives can be expressed in the necessary form, either exactly or to a close approximation [1]. Many relationships that cannot be formulated exactly as posynomials can be approximated closely, using methods for fitting GP-compatible models to data [10].

B. Signomial Programming

Geometric programming is a powerful tool, with strong guarantees. As discussed above, however, the formulation can prove restrictive. While changes of variable present an elegant way of circumventing some formulation obstacles, there may not always exist a suitable variable change. In particular, the restriction $c > 0$ in the definition of a posynomial can be a prohibitive obstacle for a modeler. There are many models where being able to use a negative monomial term is critical. An example of this is if we want to minimize the difference between two quantities.

A *signomial* is a function with the same form as a posynomial,

$$s(\mathbf{u}) = \sum_{k=1}^K c_k \prod_{j=1}^n u_j^{a_{jk}}, \tag{4}$$

except that the coefficients, $c_k \in \mathbb{R}$, can now be any real number. In particular, they can be non-positive. A signomial program is therefore a generalization of a geometric program, where the constraint functions can be signomials^b:

$$\begin{aligned}
& \text{minimize} && p_0(\mathbf{u}) \\
& \text{subject to} && s_i(\mathbf{u}) \leq 0, \quad i = 1, \dots, n_s, \\
& && p_i(\mathbf{u}) \leq 1, \quad i = 1, \dots, n_p, \\
& && m_i(\mathbf{u}) = 1, \quad i = 1, \dots, n_m.
\end{aligned} \tag{5}$$

An important point is that *adding just one signomial constraint to a geometric program with arbitrarily many posynomial constraints changes the geometric program to a signomial program*.

The bad news is that the increased expressiveness of signomial programming comes at a price: we can no longer guarantee a *global* optimum, because, unlike with GP, the log transformation of a signomial program is not a convex optimization problem.

The good news is that there is a disciplined method for solving **Signomial Programs (SPs)**. A locally optimal solution can be found by solving a sequence of GPs [2], where at each iteration a local GP approximation to the SP is solved, until convergence is achieved. Signomial programming is an example of ‘difference of convex’ programming, because the logarithmically-transformed problem can be expressed as

$$\begin{aligned}
& \text{minimize} && f_0(x) \\
& \text{subject to} && f_i(x) - g_i(x) \leq 0, \quad i = 1, \dots, m
\end{aligned} \tag{6}$$

where f_i and g_i are convex. This means that, for the convex (GP) approximation, $\hat{f}(x)$, of the non-convex (SP) function, $f(x) - g(x)$,

$$\hat{f}(x) \geq f(x) \quad \forall x. \tag{7}$$

Because of this, the true feasible set contains the feasible set of the convexified problem, and there is no need for a trust region [11], meaning that there is no need to tune solver parameters for controlling initial trust region sizes and/or update rules. Solving an SP is, therefore, considerably more reliable than solving a general nonlinear program, as there are fewer solver algorithm parameters to tune.

C. Terminology

Before further discussion, it is useful to introduce some of the vocabulary used to describe this work.

^bThe fact that signomial constraints are expressed as being less than or equal to zero (as opposed to 1) is a subtlety of SP solution algorithms that allows for a more efficient solution heuristic.

1. Models

In the context of this work a *model* is a list of constraints, usually accompanied by an objective function. The objectives and constraints are composed of design variables, which are the outputs of the model, and fixed variables or constants, which are inputs to the model. Occasionally the term model may also refer to a list of constraints without an explicit objective function.

2. GP- and SP-compatibility

A constraint is described as being *GP-compatible* if it can be written in the form of either the inequality or equality constraints in (3). By extension, a *GP-compatible* model is one where the design variables, objectives, and constraints all satisfy the requirements of a GP (3). If a model does not satisfy the requirements of being a GP, but satisfies the slightly more relaxed requirements of an *SP* (5), it is said to be *SP-compatible*.

3. Parent and Child Models

A parent model is a model that adopts one or more self-contained child models. Both parent and child models are typically self-standing, meaning they have their own objective functions and are both primal- and dual-feasible. When a parent model adopts a child model, however, its objective function supersedes that of the child model. A model can be both a parent model and a child model and the highest level parent model's objective function governs the final composed model.

Because models are effectively lists of constraints, model composition is little more than concatenation of these lists. If both the parent model and the child model are *GPs*, i.e. can be logarithmically transformed into convex optimization problems, then the composition of the models together can be thought of as the intersection of two log-convex feasible sets, which is itself log-convex.

The use of modular parent and child models is helpful both from the practical perspective of code organization, and from the perspective of being able to cleanly use and maintain the same child model in multiple parent models. For example, for a relatively simple analysis, a wing and tail can share the same structural model. This modularity means that a structural model can then be enhanced or even replaced with a better model easily.

III. Method

GPkit [12] is a tool that has recently been developed at MIT to enable fast formulation and solution of *GPs*. GPkit interfaces with both open-source and commercially-available interior point method solvers. For the purpose of this work, we use MOSEK [13] with a free academic license.

Recent work by Hoburg and Burnell has extended the capabilities of GPkit in two key areas: (i) the ability to formulate signomial programs, and a sequential GP heuristic for solving them, and (ii) a framework to facilitate model composition of parent and child models, using modular model structures and simple, readable syntax.

IV. Subsystem Models

Building on previous work, and given the need for higher fidelity modeling of aircraft subsystems, the main contributions of this work are *SP-compatible* subsystem models for a commercial subsonic transport aircraft with a tube-and-wing configuration. Specifically, the models are for the vertical tail, fuselage, and landing gear. The purpose of these models is to determine optimal sizing of each system for a fixed configuration, as opposed to being a more general conceptual design exploration tool. Generalizing these models to allow for unconventional configurations is beyond the scope of this work.

For each of these models, the objective functions are placeholders for more specific objective functions that would be defined by a higher level model. For example, the highest level objective might be to minimize the total operating cost of an aircraft, which would apply downward pressure on subsystem weight and drag, where applicable.

As a verification method, the Boeing 737 MAX is used as a benchmark aircraft against which to test the models. Model inputs are based on true Boeing 737 MAX values wherever possible [14, 15] and estimated where the values are unknown, with the intention of comparing the resulting solution to the true aircraft design. The Boeing 737 MAX is chosen because it is the newest version of the most prolific narrowbody commercial aircraft in the world.

A. Vertical Tail

The purpose of an aircraft's vertical tail is two-fold. Firstly, it must provide stability in yaw. Secondly, it must provide adequate yaw control authority in critical flight conditions. For a multi-engine aircraft, the critical flight condition is

typically an engine failure at low speeds. The vertical tail must be capable of providing sufficient sideforce in this case [16]. The design of the vertical tail is therefore coupled to the size of the fuselage and the position of the engines, and this is captured by the model.

1. Model assumptions

The high level assumptions for this model are that the aircraft has a single vertical tail, the horizontal tail is mounted in a conventional configuration, so as to not require a reinforced vertical tail structure, and the aircraft has two wing-mounted engines. This model also assumes that the ultimate high level model's objective (e.g. minimizing fuel consumption or operating costs) would apply downward pressure on both weight and drag.

2. Model description

Table 1: Vertical tail model free variables

Free Variables	Units	Description
Vertical Tail		
A_{vt}	[-]	Vertical tail aspect ratio
$C_{D_{vis}}$	[-]	Viscous drag coefficient
$C_{L_{vt}}$	[-]	Vertical tail lift force coefficient
D_{vis}	[N]	Vertical tail viscous drag in cruise
D_{wm}	[N]	Engine out windmill drag
L_{max}	[N]	Maximum load for structural sizing
L_{vt}	[N]	Vertical tail lift in engine out condition
Re_c	[-]	Vertical tail Reynolds number in cruise
S	[m ²]	Vertical tail reference area (full span)
S_{vt}	[m ²]	Vertical tail reference area (half span)
W_{struct}	[N]	Full span weight (from structural model)
W_{vt}	[N]	Vertical tail weight
Δx_{lead}	[m]	Distance from CG to vertical tail leading edge
Δx_{trail}	[m]	Distance from CG to vertical tail trailing edge
λ	[-]	Vertical tail taper ratio
τ	[-]	Vertical tail thickness to chord ratio
b	[m]	Vertical tail full span
b_{vt}	[m]	Vertical tail half span
\bar{c}	[m]	Vertical tail mean aerodynamic chord
c_{root}	[m]	Vertical tail root chord
c_{tip}	[m]	Vertical tail tip chord
l_{vt}	[m]	Vertical tail moment arm
p	[-]	Substituted variable = $1 + 2\lambda$
q	[-]	Substituted variable = $1 + \lambda$
$z_{\bar{c}}$	[m]	Vertical location of the mean aerodynamic chord
Vertical Tail Structure (duplicate variables linked)		
A	[-]	Aspect ratio
I_{cap}	[-]	Non-dim. spar cap area moment of inertia
L_{max}	[N]	Maximum load for structural sizing
M_r	[N]	Root moment per root chord
S	[m ²]	Reference area
W_{cap}	[N]	Weight of spar caps
W_{struct}	[N]	Structural weight
W_{web}	[N]	Weight of shear web
λ	[-]	Vertical tail taper ratio
ν	[-]	Substituted variable = $(\lambda^2 + \lambda + 1)/(\lambda + 1)$
τ	[-]	Thickness to chord ratio
b	[m]	Span
p	[-]	Substituted variable = $1 + 2\lambda$
q	[-]	Substituted variable = $1 + \lambda$
t_{cap}	[-]	Non-dim. spar cap thickness
t_{web}	[-]	Non-dim. shear web thickness

Table 2: Vertical tail model constants

Constants	Units	Description
-----------	-------	-------------

Vertical Tail

A_{eng}	$[m^2]$	Engine reference area
$C_{D_{wm}}$	$[-]$	Windmill drag coefficient
$C_{L_{vmax}}$	$[-]$	Max lift coefficient for structural sizing
L_{fuse}	$[m]$	Length of fuselage
T_e	$[N]$	Thrust per engine at takeoff
V_1	$[m/s]$	Minimum takeoff velocity
V_c	$[m/s]$	Cruise velocity
V_{ne}	$[m/s]$	Never exceed velocity for structural sizing
μ	$[N * s/m^2]$	Dynamic viscosity (35,000ft)
ρ_c	$[kg/m^3]$	Air density at cruise (35,000ft)
ρ_{TO}	$[kg/m^3]$	Air density at takeoff (sea level)
$\tan(\Lambda_{LE})$	$[-]$	Tangent of leading edge sweep (40 deg)
$c_{l_{vt}}$	$[-]$	Sectional lift force coefficient (engine out)
e	$[-]$	Span efficiency of vertical tail
l_e	$[m]$	Engine moment arm
x_{CG}	$[m]$	x-location of CG

Vertical Tail Structure

N_{lift}	$[-]$	Wing loading multiplier
ρ_{cap}	$[kg/m^3]$	Density of spar cap material
ρ_{web}	$[kg/m^3]$	Density of shear web material
$\sigma_{max, shear}$	$[Pa]$	Allowable shear stress
σ_{max}	$[Pa]$	Allowable tensile stress
$f_{w, add}$	$[-]$	Wing added weight fraction
g	$[m/s^2]$	Gravitational acceleration
r_h	$[-]$	Fractional wing thickness at spar web
w	$[-]$	Wingbox-width-to-chord ratio

The placeholder objective function for the vertical tail model is a somewhat arbitrary function of cruise viscous drag and weight, and is intended to reflect how a higher level objective might apply pressure to the vertical tail model.

$$D_{vis} + 0.1W_{vt} \quad (8)$$

The first constraint specifies that the maximum moment exerted by the tail must be greater than or equal to the moment exerted by the engines in an engine-out condition. In the worst case scenario, not only is there an asymmetric thrust but this is exacerbated by the windmill drag of the engine that is shut off [5].

$$L_{vt}l_{vt} \geq D_{wm}l_e + T_e l_e \quad (9)$$

The moment arm of the vertical tail is the distance from the aircraft **Center of Gravity (CG)** to the aerodynamic center of the vertical tail, which is assumed to be at the quarter chord. The moment arm is therefore upper bounded by the distance from the **CG** to the leading edge of the tail at the root, the height of the mean aerodynamic chord above the fuselage, the sweep angle, and the mean aerodynamic chord.

$$\Delta x_{lead} + z_{\bar{c}} \tan(\Lambda_{LE}) + 0.25\bar{c} \geq l_{vt} \quad (10)$$

Note that this is a signomial constraint. A simple **GP**-compatible approximation to this constraint would be to neglect sweep and to assume that the aerodynamic center is at the leading edge.

The worst case engine out condition is likely to occur during takeoff, when the velocity is lowest but the engine force required to safely complete takeoff is highest. The force exerted by the vertical tail in this critical low speed case is determined as the maximum lift coefficient of the tail and vertical tail reference area multiplied by the minimum dynamic pressure, which might typically occur at the rotation speed at sea level. As a conservative estimate, the V_1 speed is used because it is the minimum speed after which a takeoff can be completed, following a critical engine failure. This constraint can be made more demanding by assuming a high altitude runway.

$$L_{vt} = \frac{1}{2}\rho_0 V_1^2 S_{vt} C_{L_{vt}} \quad (11)$$

Using finite wing theory, the 3D lift coefficient can be related to the airfoil sectional lift coefficient by the following relationship [18]:

$$C_{L_{vt}} \left(1 + \frac{c_{l_{vt}}}{\pi e A_{vt}} \right) \leq c_{l_{vt}} \quad (12)$$

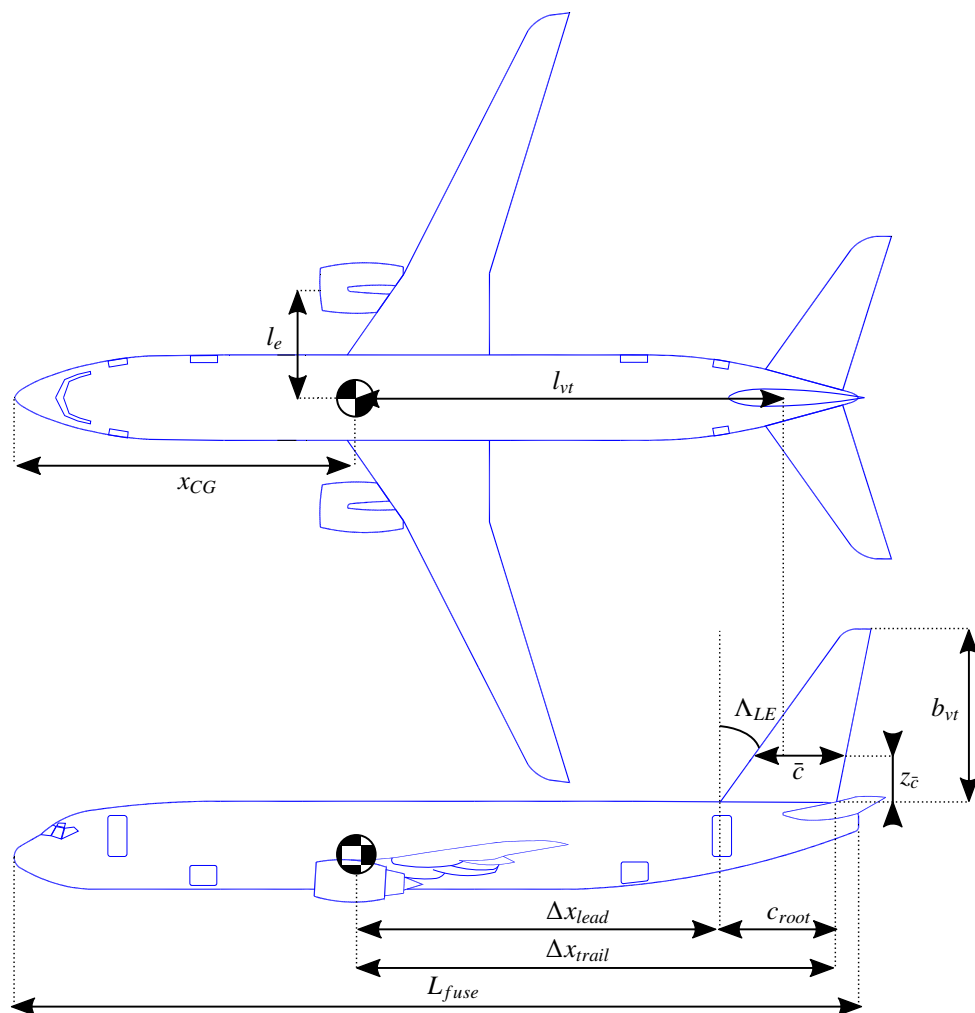


Figure 1: Key dimensions for the vertical tail model (adapted from [17])

Meanwhile, the windmill drag can, to a first approximation, be calculated using a drag coefficient and a reference area [5], in this case the area of the engine fan.

$$D_{wm} \geq \frac{1}{2} \rho_0 V_1^2 A_{eng} C_{D_{wm}} \quad (13)$$

A simple formula relates the reference area, span and mean geometric chord, for a trapezoidal tail. This is another signomial constraint.

$$S_{vt} \leq b_{vt} \frac{c_{root} + c_{tip}}{2} \quad (14)$$

To further define the geometry of the vertical tail, the x-coordinates of the leading and trailing edge at the root are related by the root chord. The tail trailing edge is upper bounded by imposing a constraint that the tail root cannot extend beyond the end of the fuselage. Together these constraints put an upper bound on the moment arm of the tail based on the length of the fuselage.

$$\Delta x_{trail} \geq c_{root} + \Delta x_{lead} \quad (15)$$

$$L_{fuse} \geq x_{CG} + \Delta x_{trail} \quad (16)$$

The mean aerodynamic chord for a trapezoidal wing is defined as:

$$\bar{c} = \frac{2}{3} \left(\frac{1 + \lambda + \lambda^2}{1 + \lambda} \right) c_{root} \quad (17)$$

This can be made into a signomial constraint. Though not absolutely necessary, substitute variables p and q already appear in the structural sub-model and are therefore convenient to use here too.

$$\bar{c} \leq \frac{2}{3} \left(\frac{1 + \lambda + \lambda^2}{q} \right) c_{root} \quad (18)$$

$$2q \geq 1 + p \quad (19)$$

$$p \geq 1 + 2\lambda \quad (20)$$

$$\lambda = \frac{c_{tip}}{c_{root}} \quad (21)$$

One advantage of using these posynomial constraint substitutions is that they can be reused for the constraint that defines the vertical position of the mean aerodynamic chord, which saves us from needing to implement another signomial constraint.

$$z_{\bar{c}} = \frac{b_{vt} q}{3p} \quad (22)$$

It is necessary put a lower bound on taper to avoid unacceptably small Reynolds numbers at the tip [19]. For the purpose of this work, the taper is lower bounded by the taper ratio of the benchmark aircraft [15].

$$\lambda \geq 0.27 \quad (23)$$

The viscous drag for the tail in cruise is lower bounded using the familiar expression for drag. A GP-compatible fitted model [20] is used to capture the dependence on airfoil thickness and Reynolds number based on the mean aerodynamic chord. 50 data points were sampled using XFOIL [21] and a posynomial constraint was then fitted to these data points.

$$D_{vis} \geq \frac{1}{2} \rho_c V_c^2 S_{vt} C_{D_{vis}} \quad (24)$$

$$C_{D_{vis}}^{0.12} \geq 0.118 Re_c^{0.0016} \tau^{0.0082} + 0.198 Re_c^{0.0017} \tau^{0.0077} + 0.19 Re_c^{0.0017} \tau^{0.0075} + 1.83 \times 10^4 \frac{\tau^{3.5}}{Re_c^{0.49}} \quad (25)$$

$$Re_c = \frac{\rho_c V_c \bar{c}}{\mu} \quad (26)$$

Finally, the tail model adopts the wing structure model from Hoburg [1], which adds a further 12 constraints. This structural model requires a maximum load, which is constrained by a maximum dynamic pressure and a maximum lift coefficient.

$$L_{max} = \frac{1}{2} \rho_0 V_{ne}^2 S_{vt} C_{L_{max}} \quad (27)$$

The wing structure model is for a full span wing, whereas, naturally, the vertical tail only has a “half” span. For this reason the vertical tail geometry and weight must be related to the geometry and weight definitions used in the structural model.

$$2S_{vt} = S \quad (28)$$

$$2b_{vt} = b \quad (29)$$

$$2W_{vt} = W_{struct} \quad (30)$$

3. Model Results

By using fixed values representative of the benchmark aircraft, a solution was obtained for this SP. Tables of the optimal values and the constant values used can be found in the appendix. Solving the SP took 4 GP solves and 0.48 seconds. There is reasonable agreement between the optimal values and the values for the benchmark aircraft as can be seen in Table 3.

Table 3: Solution comparison with the benchmark aircraft

Design Variable	Value	Estimate for benchmark aircraft
A_{vt} [-]	1.81	1.91 [15]
b_{vt} [m]	7.56	7.16 [15]
S_{vt} [m ²]	31.6	26.4 [15]

The objective function value is most sensitive to the length of the fuselage: a 1% decrease in the fuselage length would undesirably increase the objective function value by approximately 2.8%. The next most influential parameter is the worst-case velocity for which the tail must be able to handle the engine out condition. According to this model, if the V_1 speed is decreased by 1%, the objective value would increase by 2.5%. The objective function is also sensitive to the cruise velocity, the x-location of the CG, and the spanwise position of the engine. Decreasing these parameters by 1% would decrease the objective value by 1.4%, 1.3%, and 1.3%, respectively.

B. Fuselage

At a high level, the purpose of a conventional commercial aircraft fuselage can be decomposed into two primary functions: integrating and connecting all of the subsystems (e.g. wing, tail, landing gear), and carrying the payload, which typically consists of passengers, luggage, and sometimes cargo. The design of the fuselage is therefore coupled with virtually every aircraft subsystem, and the tail and landing gear are no exception.

Drela performs a detailed, but still approximate, analysis of fuselage structure and weight in [5], considering pressure loads, torsion loads, buoyancy weight, window weight, payload proportional weights, the floor, the tail cone, and bending loads. The majority of the constraints in this model are adapted directly from these equations.

1. Model assumptions

This model assumes a single circular cross section fuselage. This is slightly inaccurate for narrowbody aircraft like the Boeing 737 and Airbus A320, neither of which have perfectly circular cross sections. The model also assumes a single vertical tail with a conventional configuration, and a single aisle. It also assumes that a higher level model dictates an optimal number of passengers, and again, that drag and weight are both undesirable.

2. Model description

Table 4: Fuselage model free variables

Free Variables	Units	Description
A_{floor}	[m ²]	Floor beam cross sectional area
A_{fuse}	[m ²]	Fuselage cross sectional area
A_{hold}	[m ²]	Cross sectional area of the hold
A_{skin}	[m ²]	Skin cross sectional area
D	[N]	Total drag in cruise
$D_{friction}$	[N]	Friction drag
$D_{upsweep}$	[N]	Form drag due to fuselage upsweep

FF	$[-]$	Fuselage form factor
M_{floor}	$[N * m]$	Maximum bending moment in floor beams
P_{floor}	$[N]$	Distributed floor load
Q_v	$[N * m]$	Torsion moment imparted by vertical tail
R_{fuse}	$[m]$	Fuselage radius
S_{bulk}	$[m^2]$	Bulkhead surface area
S_{floor}	$[N]$	Maximum shear in floor beams
S_{nose}	$[m^2]$	Nose surface area
V_{bulk}	$[m^3]$	Bulkhead skin volume
V_{cabin}	$[m^3]$	Cabin volume
V_{cargo}	$[m^3]$	Cargo volume
V_{cone}	$[m^3]$	Cone skin volume
V_{cyl}	$[m^3]$	Cylinder skin volume
V_{floor}	$[m^3]$	Floor volume
V_{hold}	$[m^3]$	Hold volume
$V_{luggage}$	$[m^3]$	Luggage volume
V_{nose}	$[m^3]$	Nose skin volume
W_{apu}	$[N]$	APU weight
W_{buoy}	$[N]$	Buoyancy weight
W_{cone}	$[N]$	Cone weight
W_{floor}	$[N]$	Floor weight
W_{fuse}	$[N]$	Fuselage weight
W_{insul}	$[N]$	Insulation material weight
$W_{luggage}$	$[N]$	Passenger luggage weight
W_{padd}	$[N]$	Misc. weights (attendants, food, galley, toilets, doors etc.)
W_{pass}	$[N]$	Passenger weight
W_{pay}	$[N]$	Payload weight
W_{seat}	$[N]$	Seating weight
W_{shell}	$[N]$	Shell weight
W_{skin}	$[N]$	Skin weight
W_{window}	$[N]$	Window weight
λ_{cone}	$[-]$	Tailcone radius taper ratio
ϕ	$[-]$	Upsweep angle
ρ_{cabin}	$[kg/m^3]$	Air density in cabin
σ_x	$[N/m^2]$	Axial stress in skin
σ_θ	$[N/m^2]$	Hoop stress in skin
τ_{cone}	$[N/m^2]$	Shear stress in cone
f	$[-]$	Fineness ratio
h_{floor}	$[m]$	Floor I-beam height
h_{hold}	$[m]$	Height of the cargo hold
l_{cone}	$[m]$	Cone length
l_{floor}	$[m]$	Floor length
l_{fuse}	$[m]$	Fuselage length
l_{nose}	$[m]$	Nose length
l_{shell}	$[m]$	Shell length
n_{pass}	$[-]$	Number of passengers
n_{rows}	$[-]$	Number of rows
p_{λ_v}	$[-]$	$1 + 2 * \text{tail taper ratio}$
q_{λ_v}	$[-]$	$1 + \text{tail taper ratio}$
t_{cone}	$[m]$	Cone thickness
t_{shell}	$[m]$	Shell thickness
t_{skin}	$[m]$	Skin thickness
w_{floor}	$[m]$	Floor width
x_{shell1}	$[m]$	Start of cylinder section

Table 5: Fuselage model constants

Constants	Units	Description
LF	$[-]$	Load factor
L_{vmax}	$[N]$	Maximum vertical tail force
N_{land}	$[-]$	Emergency landing load factor
R	$[J/K/kg]$	Universal gas constant
S_{PR}	$[-]$	Number of seats per row
T_{cabin}	$[K]$	Cabin temperature
V_{∞}	$[m/s]$	Cruise velocity
W''_{floor}	$[N/m^2]$	Floor weight/area density
W''_{insul}	$[N/m^2]$	Weight/area density of insulation material
W'_{seat}	$[N]$	Weight per seat

W'_{window}	[N/m]	Weight/length density of windows
$W_{avg.pass}$	[lbf]	Average passenger weight
W_{cargo}	[N]	Cargo weight
$W_{carryon}$	[lbf]	Average carry-on bag weight
$W_{checked}$	[lbf]	Average checked bag weight
W_{fix}	[lbf]	Fixed weights (pilots, cockpit seats, instrumentation, navcom)
Δh	[m]	Distance from floor to widest part of fuselage
Δp	[Pa]	Pressure difference across fuselage skin
μ	[N * s/m ²]	Dynamic viscosity (35,000ft)
ρ_{∞}	[kg/m ³]	Freestream air density (35,000ft)
ρ_{bend}	[kg/m ³]	Stringer density
ρ_{cargo}	[kg/m ³]	Cargo density
ρ_{cone}	[kg/m ³]	Cone material density
ρ_{floor}	[kg/m ³]	Floor material density
$\rho_{luggage}$	[kg/m ³]	Luggage density
ρ_{skin}	[kg/m ³]	Skin density
σ_{floor}	[N/m ²]	Max allowable cap stress
σ_{skin}	[N/m ²]	Max allowable skin stress
τ_{floor}	[N/m ²]	Max allowable shear web stress
b_v	[m]	Vertical tail span
c_{vt}	[m]	Vertical tail chord
f_{apu}	[-]	APU weight as fraction of payload weight
f_{fadd}	[-]	Skin proportional added weight of local reinforcements
f_{frame}	[-]	Fractional weight of frame
$f_{lugg,1}$	[-]	Proportion of passengers with one suitcase
$f_{lugg,2}$	[-]	Proportion of passengers with two suitcases
f_{padd}	[-]	All other misc. weight as fraction of payload weight
f_{string}	[-]	Fractional weight of stringers
g	[m/s ²]	Gravitational acceleration
n_{seat}	[-]	Number of seats
p_{cabin}	[Pa]	Cabin air pressure (8000ft)
p_s	[in]	Seat pitch
r_E	[-]	Ratio of stringer/skin moduli
w_{aisle}	[m]	Aisle width
w_{seat}	[m]	Seat width
w_{sys}	[m]	Width between cabin and fuselage skin for systems/frames

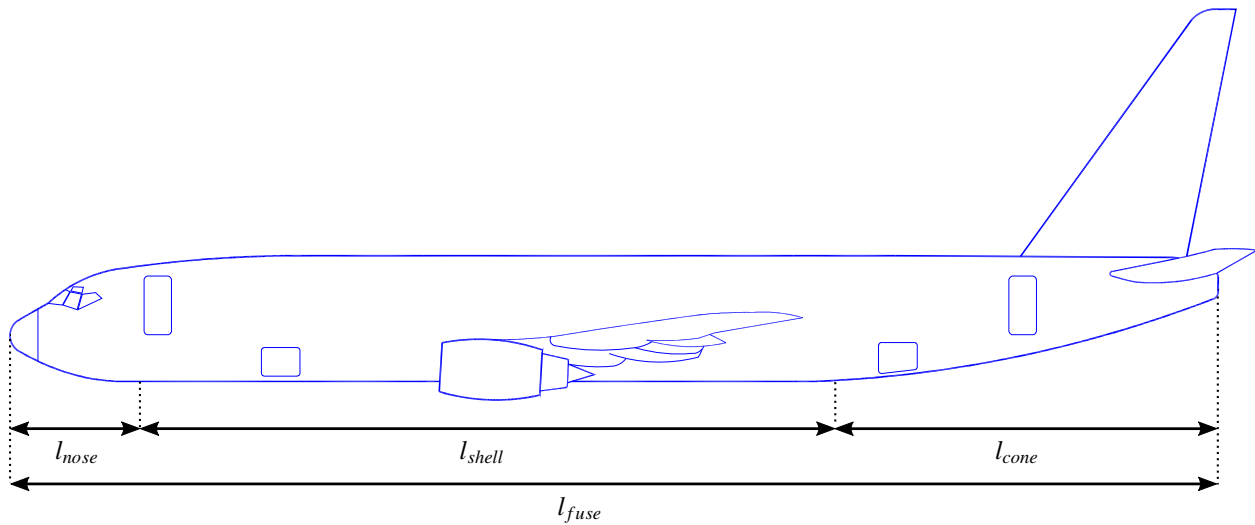


Figure 2: Key dimensions for the fuselage model (adapted from [17])

The placeholder objective is an arbitrary function of drag and weight chosen to reflect the pressure applied by a higher level objective function.

$$DW_{fuse} \quad (31)$$

The fuselage shell is assumed to begin at approximately the end of the nose section.

$$l_{nose} = x_{shell1} \quad (32)$$

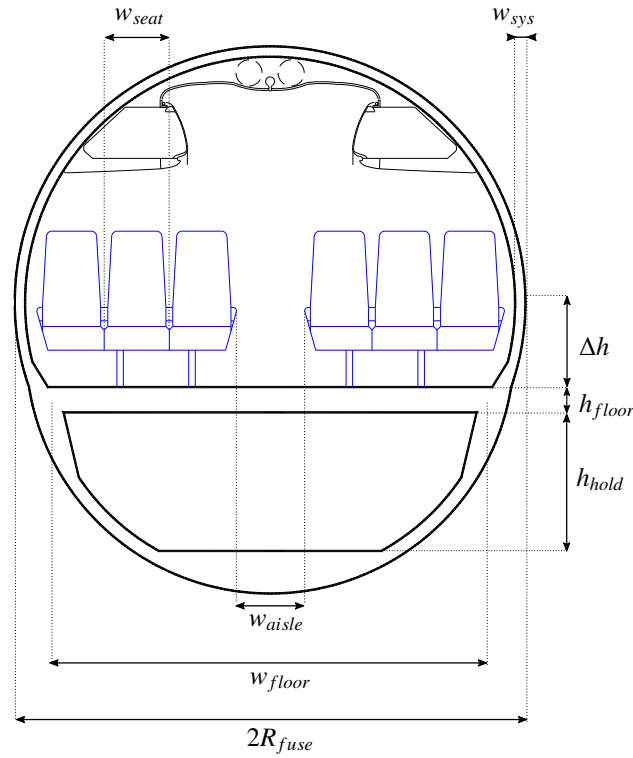


Figure 3: Key cross section dimensions for the fuselage model (adapted from [17])

The fuselage must be wide enough to accommodate the width of the seats in a row and the width of the aisle.

$$2R_{fuse} \geq (SPR)w_{seat} + w_{aisle} + 2w_{sys} \quad (33)$$

The cross sectional area of the fuselage skin is lower bounded using a thin walled cylinder assumption.

$$A_{skin} \geq 2\pi R_{fuse} t_{skin} \quad (34)$$

The cross sectional area of the fuselage is lower bounded using the radius of the fuselage.

$$A_{fuse} \geq \pi R_{fuse}^2 \quad (35)$$

The effective modulus-weight shell thickness is lower bounded by assuming that only the skin and stringers contribute to bending. This constraint also uses an assumed fractional weight of stringers that scales with the thickness of the skin.

$$t_{shell} \geq t_{skin} \left(1 + f_{string} r_E \frac{\rho_{skin}}{\rho_{bend}} \right) \quad (36)$$

The axial and hoop stresses in the fuselage skin are calculated based on the pressurization load due to the difference between cabin pressure and ambient pressure at cruise altitude. The thickness of the skin is therefore sized by the maximum allowable stress of the chosen material.

$$\sigma_x = \frac{\Delta p R_{fuse}}{2 t_{shell}} \quad (37)$$

$$\sigma_\theta = \Delta p \frac{R_{fuse}}{t_{skin}} \quad (38)$$

$$\sigma_{skin} \geq \sigma_x \quad (39)$$

$$\sigma_{skin} \geq \sigma_\theta \quad (40)$$

With the skin thickness constrained we can assert a lower bound for the weight of the fuselage skin, excluding the tail cone. This is done by calculating the volume of the skin for the nose, main cabin, and rear bulkhead, and then

multiplying this by the skin material density. The surface area of the nose, which is approximated as an ellipse, is calculated using Cantrell's approximation [5]. The surface area of the hemispherical rear bulkhead is also constrained.

$$S_{nose} \geq (2\pi R_{fuse}^2)^{\frac{2}{3}} \left(\frac{1}{3} + \frac{2}{3} \left(\frac{l_{nose}}{R_{fuse}} \right)^{\frac{2}{3}} \right) \quad (41)$$

$$S_{bulk} = 2\pi R_{fuse}^2 \quad (42)$$

$$V_{cyl} = A_{skin} l_{shell} \quad (43)$$

$$V_{nose} = S_{nose} t_{skin} \quad (44)$$

$$V_{bulk} = S_{bulk} t_{skin} \quad (45)$$

$$W_{skin} \geq \rho_{skin} g (V_{bulk} + V_{cyl} + V_{nose}) \quad (46)$$

The weight of the fuselage shell is then constrained by accounting for the weights of the frame, stringers, and other structural components, all of which are assumed to scale with the weight of the skin.

$$W_{shell} \geq W_{skin} (1 + f_{fadd} + f_{frame} + f_{string}) \quad (47)$$

The effective buoyancy weight of the aircraft is also calculated using a specified cabin pressure at cruise, the ideal gas law, an approximate cabin volume, and the difference in pressure with respect to the ambient pressure at cruise.

$$\rho_{cabin} = \frac{P_{cabin}}{RT_{cabin}} \quad (48)$$

$$V_{cabin} \geq A_{fuse} (0.67R_{fuse} + 0.67l_{nose} + l_{shell}) \quad (49)$$

$$W_{buoy} \geq (\rho_{cabin} - \rho_{\infty}) g V_{cabin} \quad (50)$$

The window and insulation weight is calculated using assumed weight/length and weight/area densities respectively. It is assumed that only the cabin is insulated and that the cabin takes up approximately 55% of the fuselage cross section.

$$W_{window} = W'_{window} l_{shell} \quad (51)$$

$$W_{insul} \geq W''_{insul} (0.55 (S_{bulk} + S_{nose}) + 1.1\pi R_{fuse} l_{shell}) \quad (52)$$

The APU is assumed to be proportional to the payload weight. Other payload proportional weight is also accounted for using a weight fraction. This category includes flight attendants, food, galleys, toilets, furnishing, doors, lighting, air conditioning, and in-flight entertainment systems. The total seat weight is a product of the weight per seat and the number of seats.

$$W_{apu} = W_{pay} f_{apu} \quad (53)$$

$$W_{padd} = W_{pay} f_{padd} \quad (54)$$

$$W_{seat} = W'_{seat} n_{seat} \quad (55)$$

The floor must be designed to withstand at least the weight of the payload and seats multiplied by a safety factor for an emergency landing.

$$P_{floor} \geq N_{land} W_{pay} + N_{land} W_{seat} \quad (56)$$

The maximum moment and shear in the floor are determined based on this design load and the width of the floor, assuming that the floor/wall joints are pinned and there are no center supports.

$$S_{floor} = 0.5P_{floor} \quad (57)$$

$$M_{floor} = 0.125P_{floor} W_{floor} \quad (58)$$

The length of the nose is lower bounded by a fixed value necessary for the cockpit length.

$$l_{nose} \geq 5.2[m] \quad (59)$$

The floor beam cross sectional area is constrained by the maximum allowable cap stress and shear web stress for the beams.

$$A_{floor} \geq 1.5 \frac{S_{floor}}{\tau_{floor}} + 2 \frac{M_{floor}}{\sigma_{floor} h_{floor}} \quad (60)$$

The seat pitch and the number of rows are fixed and constrain the length of the shell. Meanwhile, the required height from the widest part of the fuselage to the floor constrains the width of the floor. Such a constraint could reflect a passenger comfort metric or even a window viewing angle requirement.

$$l_{shell} \geq n_{rows} p_s \quad (61)$$

$$l_{floor} \geq 2R_{fuse} + l_{shell} \quad (62)$$

$$\left(\frac{W_{floor}}{2}\right)^2 + \Delta h^2 \geq R_{fuse}^2 \quad (63)$$

The weight of the floor is therefore lower bounded by a density of the floor beams multiplied by the volume in addition to an assumed weight/area density for the planking.

$$V_{floor} \geq A_{floor} W_{floor} \quad (64)$$

$$W_{floor} \geq V_{floor} \rho_{floor} g + W''_{floor} l_{floor} W_{floor} \quad (65)$$

The tail cone needs to be able to transfer the loads exerted on the vertical tail to the rest of the fuselage. The maximum torsion moment imparted by the vertical tail depends on the maximum force exerted on the tail as well as the span and taper ratio of the tail.

$$Q_v = \frac{L_{vmax} b_v}{3} \frac{1 + 2\lambda_v}{1 + \lambda_v} \quad (66)$$

Although this is already a signomial constraint and could be left as is, a change of variables is used for future compatibility with the structural sub-model within the tail model, which uses $p = 1 + 2\lambda_v$ and $q = 1 + \lambda_v$ to make a structural constraint GP compatible. The same taper lower bound is introduced as in the tail model.

$$Q_v = \frac{L_{vmax} b_v}{3} \frac{p_{\lambda_v}}{q_{\lambda_v}} \quad (67)$$

$$1 + p_{\lambda_v} \geq 2q_{\lambda_v} \quad (68)$$

$$p_{\lambda_v} \geq 1.6 \quad (69)$$

The cone skin shear stress is constrained to the maximum allowable stress in the skin material.

$$\tau_{cone} = \sigma_{skin} \quad (70)$$

The thickness of the cone skin is constrained by the torsion moment, the cone cross sectional area, and the maximum shear stress of the cone materials. The cone cross sectional area, which of course varies along the cone, is coarsely approximated to be the fuselage cross sectional area, i.e. the cross sectional area of the cone base.

$$Q_v = 2A_{fuse} \tau_{cone} t_{cone} \quad (71)$$

The volume of the cone is a definite integral from the base to the tip of the cone. This integral is evaluated in [5] and rearranged into a signomial constraint.

$$R_{fuse} V_{cone} (1 + \lambda_{cone}) \geq 2 \frac{Q_v l_{cone}}{\tau_{cone}} \quad (72)$$

The tail cone taper ratio, defined as the ratio of the cone radius at the leading edge of the tail and the radius at the base of the cone (i.e. the fuselage radius), is specified. Ideally this would be a design variable, however, leaving it unspecified results in a dual infeasible problem. TASOPT requires the taper ratio to be fixed as well.

$$\lambda_{cone} = 0.4 \quad (73)$$

This taper ratio constrains the length of the cone relative to the chord of the tail (approximated as the mean aerodynamic chord), which is fixed.

$$\lambda_{cone} = \frac{c_{vt}}{l_{cone}} \quad (74)$$

Just like the shell, the cone weight is bounded using assumed proportional weights for additional structural elements, stringers, and frames.

$$W_{cone} \geq \rho_{cone} g V_{cone} (1 + f_{fadd} + f_{frame} + f_{string}) \quad (75)$$

The passenger component of payload weight depends on load factor.

$$n_{seat} = (SPR)n_{rows} \quad (76)$$

$$n_{pass} = (LF)n_{seat} \quad (77)$$

$$W_{pass} = W_{avperson}n_{pass} \quad (78)$$

The weight of luggage is lower bounded by a buildup of 2-checked-bag customers, 1-checked-bag customers, and average carry-on weight. This constraint is disproportionately and unnecessarily detailed, but it serves to demonstrate that constraints of a posynomial form can be made arbitrarily complex for little additional cost, as discussed earlier.

$$W_{luggage} \geq 2W_{checked,flugg,2}n_{pass} + W_{checked,flugg,1}n_{pass} + W_{carryon} \quad (79)$$

The weight of luggage and cargo is of course tied to the volume and average density of luggage and cargo. The volume determined by these constraints can be used to determine required luggage hold volume, which in turn helps to determine the hold cross sectional area.

$$W_{luggage} = V_{luggage}\rho_{luggage}g \quad (80)$$

$$W_{cargo} = V_{cargo}\rho_{cargo}g \quad (81)$$

$$V_{hold} \geq V_{cargo} + V_{luggage} \quad (82)$$

$$V_{hold} = A_{hold}l_{shell} \quad (83)$$

Given the required cargo hold cross sectional area, and the fact that the cargo hold shape is approximately a segment of the circular cross section, we can constrain the required hold height using an approximation of the area of a circle segment developed by Harris [22]. This approximation is conveniently in **SP** form and is guaranteed to be within 0.1% of the true value for arc angles less than 150° and within 0.8% for all other angles.

$$A_{hold} \leq \frac{1}{2} \frac{h_{hold}^3}{w_{floor}} + \frac{2}{3} h_{hold} w_{floor} \quad (84)$$

This hold height introduces another constraint on the height of the floor beams and the radius of the fuselage cross section, given a required vertical distance from the floor to the widest part of the fuselage, in the interest of passenger comfort.

$$R_{fuse} \geq \Delta h + h_{floor} + h_{hold} \quad (85)$$

The total weight of the payload, and in turn the total weight of the fuselage, can be determined by adding all of the constituent weights. The fixed weight incorporates pilots, cockpit windows, cockpit seats, flight instrumentation, navigation and communication equipment, which are expected to be roughly the same for all aircraft [5].

$$W_{pay} \geq W_{cargo} + W_{luggage} + W_{pass} \quad (86)$$

$$W_{fuse} \geq W_{apu} + W_{buoy} + W_{cone} + W_{floor} + W_{insul} + W_{padd} + W_{seat} + W_{shell} + W_{window} + W_{fix} \quad (87)$$

The drag felt by the fuselage in cruise is approximated using a form factor, which is a function of the fineness ratio [16].

$$l_{fuse} \geq l_{nose} + l_{shell} + l_{cone} \quad (88)$$

$$f = \frac{l_{fuse}}{\sqrt{\left(\frac{4}{\pi}\right)A_{fuse}}} \quad (89)$$

$$FF \geq 1 + \frac{60}{f^3} + \frac{f}{400} \quad (90)$$

A lower bound approximation for the friction drag is then the form factor multiplied by the integral of the turbulent flat plate skin friction coefficient [18] over a cylinder. A simplistic assumption here is the lack of correction for compressibility effects.

$$D_{friction} \geq (FF) \left(2\pi R_{fuse}\right) \left(\frac{1}{2}\rho V_{\infty}^2\right) \left(0.074 \frac{\nu}{V_{\infty}} Re^{0.8}\right)$$

$$\Rightarrow D_{friction} \geq 0.074\pi(FF)R_{fuse}\mu V_{\infty} \left(\frac{\rho_{\infty} V_{\infty} l_{fuse}}{\mu} \right)^{0.8}$$

An additional source of fuselage drag can be parameterized by the upsweep of the fuselage, which is also coupled with the landing gear model. The upsweep angle can be related to the length of the cone and the radius of the fuselage by the tangent of the angle. Unfortunately, trigonometric functions are not SP-compatible, so we must fit it with a function that is. Fortunately, the tangent function is approximately affine in logarithmic space, so it is well approximated by a monomial function, which allows us to use an equality constraint.

$$1.13226\phi^{1.03759} = \frac{R_{fuse}}{l_{cone}} \quad (91)$$

The drag due to upsweep is approximated based on a relationship given in [16].

$$D_{upsweep} \geq (3.83A_{fuse}) \left(\frac{1}{2} \rho_{\infty} V_{\infty}^2 \right) \phi^{2.5} \quad (92)$$

The total drag is lower bounded by the drag due to friction and the drag due to upsweep.

$$D \geq D_{friction} + D_{upsweep} \quad (93)$$

3. Model Results

By using fixed values representative of the benchmark aircraft, a solution was obtained for this SP. Tables of the optimal values and the constant values used can be found in the appendix. Solving the SP took 5 GP solves and 0.51 seconds. Again, there is reasonable agreement between the optimal values and the values for the benchmark aircraft, which are estimated using [5, 14].

Table 6: Solution comparison with the benchmark aircraft

Design Variable	Value	Estimate for benchmark aircraft
R_{fuse} [m]	1.86	1.88 [14]
l_{fuse} [m]	39.6	39.1 [14]
W_{fuse} [kg]	15,100	16,300 [5]

The objective function is most sensitive to seat width: a 1% decrease in seat width would yield approximately a 2.2% improvement (decrease) in the objective. The objective function is also sensitive to the cruise velocity (1.9%), the number of seats per row (1.8%), and the total number of seats (1.1%). Of course, the fact that the last two quantities must be an integer and a multiple of the number of seats per row, respectively must be taken into consideration. Interestingly, the next most influential parameter is the tail chord. According to this model, a 1% decrease in the tail chord would undesirably increase the objective function value by 0.9%.

C. Landing Gear

The landing gear is integral to the configuration of the aircraft. Its purpose is to support the weight of the aircraft and allow it to manoeuvre while it is on the ground, including during taxi, takeoff, and landing. The landing gear typically weighs between three and six percent of the maximum aircraft takeoff weight [23]. Many of the constraints imposed on landing gear design are described in [16]. MDO of landing gear is critically important because of how coupled design of the landing gear system is to other subsystems, particularly the fuselage, wings, and engine positions. Chai [23] proposes a MDO tool for landing gear design, considering the angle of pitch and roll during takeoff and landing, stability at touchdown and during taxi, sideways turnover angle, braking and steering qualities, gear length, landing gear attachment, aircraft turning radius, and centerline-guidance taxiing.

1. Model assumptions

The landing gear model assumes a conventional and retractable tricycle landing gear configuration for narrowbody commercial aircraft such as a Boeing 737 MAX. The nose gear consists of a single strut supported by two wheels. The main gear consists of two struts mounted in the inboard section of the wings, each supported by two wheels. The model only takes one CG location as an input, i.e. it does not consider CG travel. It is also assumed that the main landing gear retracts towards the centerline of the aircraft, rotating about the x axis.

2. Model description

Table 7: Landing gear model free variables

Free Variables	Units	Description
B	[m]	Landing gear base
E_{land}	[J]	Maximum kinetic energy to be absorbed in landing
F_{wm}	[-]	Weight factor (main gear)
F_{wn}	[-]	Weight factor (nose gear)
I_m	[m ⁴]	Area moment of inertia (main strut)
I_n	[m ⁴]	Area moment of inertia (nose strut)
L_m	[N]	Maximum static load through main gear
L_n	[N]	Minimum static load through nose gear
L_{ndyn}	[N]	Dynamic braking load (nose gear)
L_{wm}	[N]	Static load per wheel (main gear)
L_{wn}	[N]	Static load per wheel (nose gear)
S	[m]	Stroke of the shock absorber
T	[m]	Main landing gear track
$W_{add,m}$	[N]	Proportional added weight (main gear)
$W_{add,n}$	[N]	Proportional added weight (nose gear)
W_{lg}	[N]	Weight of landing gear
W_{mg}	[N]	Weight of main gear
W_{ms}	[N]	Weight of main struts
W_{mw}	[N]	Weight of main wheels (per strut)
W_{ng}	[N]	Weight of nose gear
W_{ns}	[N]	Weight of nose strut
W_{nw}	[N]	Weight of nose wheels (total)
$W_{wa,m}$	[lbf]	Wheel assembly weight for single main gear wheel
$W_{wa,n}$	[lbf]	Wheel assembly weight for single nose gear wheel
Δx_m	[m]	Distance between main gear and CG
Δx_n	[m]	Distance between nose gear and CG
$\tan(\phi)$	[-]	Angle between main gear and CG
$\tan(\psi)$	[-]	Tip over angle
d_{oleo}	[m]	Diameter of oleo shock absorber
d_{tm}	[in]	Diameter of main gear tires
d_{tn}	[m]	Diameter of nose tires
l_m	[m]	Length of main gear
l_n	[m]	Length of nose gear
l_{oleo}	[m]	Length of oleo shock absorber
r_m	[m]	Radius of main gear struts
r_n	[m]	Radius of nose gear struts
t_m	[m]	Thickness of main gear strut wall
t_n	[m]	Thickness of nose gear strut wall
w_{tm}	[m]	Width of main tires
w_{tn}	[m]	Width of nose tires
x_m	[m]	x-location of main gear
x_n	[m]	x-location of nose gear
x_{CG}	[m]	x-location of CG including landing gear
y_m	[m]	y-location of main gear (symmetric)

Table 8: Landing gear model constants

Constants	Units	Description
E	[GPa]	Modulus of elasticity, 4340 steel
K	[-]	Column effective length factor
N_s	[-]	Factor of safety
W_0	[N]	Weight of aircraft excluding landing gear
η_s	[-]	Shock absorber efficiency
λ	[-]	Ratio of maximum load to static load
ρ_{st}	[kg/m ³]	Density of 4340 Steel
σ_{yc}	[Pa]	Compressive yield strength, 4340 steel
$\tan(\gamma)$	[-]	Tangent of dihedral angle
$\tan(\phi_{min})$	[-]	Lower bound on ϕ
$\tan(\psi_{max})$	[-]	Upper bound on ψ
$\tan(\theta_{TO})$	[-]	Takeoff pitch angle
$d_{nacelle}$	[m]	Nacelle diameter

g	$[m/s^2]$	Gravitational acceleration
h_{hold}	$[m]$	Hold height
$h_{nacelle}$	$[m]$	Minimum nacelle clearance
n_{mg}	$[-]$	Number of main gear struts
n_{wps}	$[-]$	Number of wheels per strut
P_{oleo}	$[psi]$	Oleo pressure
w	$[ft/s]$	Ultimate velocity of descent
x_{CG_0}	$[m]$	x-location of CG excluding landing gear
x_{up}	$[m]$	Fuselage upsweep point
y_{eng}	$[m]$	Spanwise location of engines
z_{CG}	$[m]$	CG height relative to bottom of fuselage
z_{wing}	$[m]$	Height of wing relative to base of fuselage

The placeholder objective function for this model is simply the total landing gear weight, W_{lg} . This is based on the fact that having heavy landing gear directly impacts fuel consumption by increasing the empty weight of the aircraft.

The difference between the lengths of the main gear and nose gear is constrained by the vertical position of the wing with respect to the bottom of the fuselage, as well as the spanwise location of the main gear and the wing dihedral. This relationship is a signomial constraint.

$$l_n + z_{wing} + y_m \tan(\gamma) \geq l_m \quad (94)$$

The landing gear track and base are defined relative to the x- and y-coordinates of the nose and main gear.

$$T = 2y_m \quad (95)$$

$$x_m \geq x_n + B \quad (96)$$

The geometric relationships between the x-coordinates of the main gear, nose gear and the CG position must be enforced. These relationships are:

$$x_n + \Delta x_n = x_{CG} \quad (97)$$

$$x_{CG} + \Delta x_m = x_m \quad (98)$$

Because the definition of a signomial program (5) does not allow posynomial equality constraints, we must relax these to be inequality constraints. However, (97) and (98) must be satisfied exactly, meaning the constraints that enforce them must be tight. For each relationship, we have a choice between a posynomial inequality constraint and a signomial inequality constraint. As will be shown below, the load through the nose gear and main gear is proportional to the distance from the CG to the main and nose gear respectively. Because there is downward pressure on these loads - more load generally means heavier landing gear - there is also downward pressure on the distances Δx_n and Δx_m , therefore we must use a signomial constraint for both relationships.

$$x_n + \Delta x_n \geq x_{CG} \quad (99)$$

$$x_{CG} + \Delta x_m \geq x_m \quad (100)$$

Of course, the CG location is also affected by the weight and position of the landing gear, and this adds another signomial constraint.

$$(W_0 + W_{lg})x_{CG} \leq W_0 x_{CG_0} + W_{ng}x_n + W_{mg}x_m \quad (101)$$

The maximum static load through the nose and main gear is constrained by the total weight of the aircraft (excluding landing gear) and the relative distances from the CG to the main and nose gear, respectively.

$$L_n = \frac{W_0 \Delta x_m}{B} \quad (102)$$

$$L_m = \frac{W_0 \Delta x_n}{B} \quad (103)$$

For the nose gear, there is an additional dynamic load due to the braking condition. A typical braking deceleration of $3m/s^2$ is assumed [16].

$$L_{n,dyn} \geq 0.31 W_0 \frac{l_m + z_{CG}}{B} \quad (104)$$

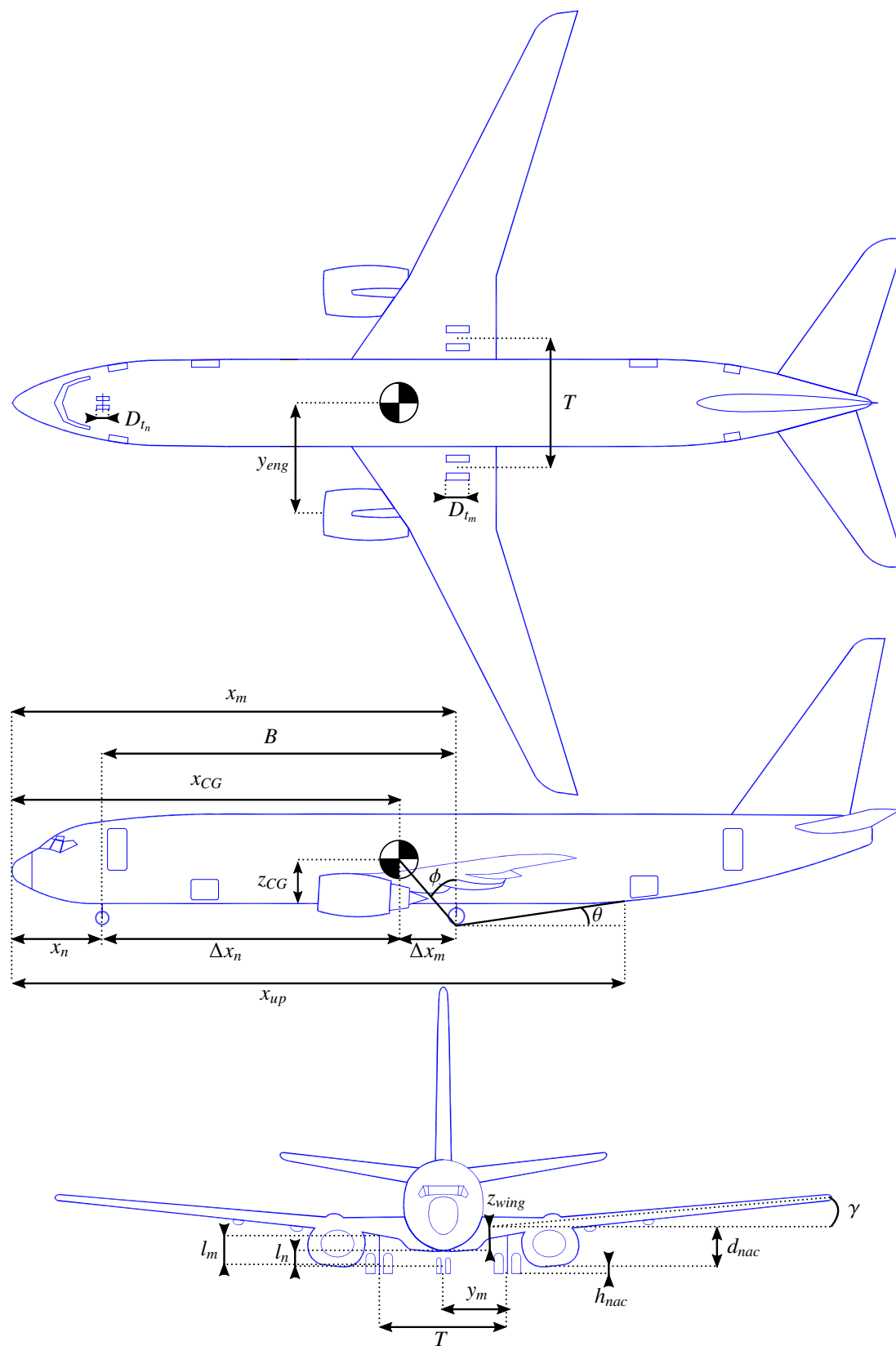


Figure 4: Key dimensions for the landing gear model (adapted from [17])

The nose gear requires adequate load for satisfactory steering performance. A typical desirable range is between 5% and 20% of the total load [16].

$$\frac{L_n}{W_0} \geq 0.05 \quad (105)$$

$$\frac{L_n}{W_0} \leq 0.2 \quad (106)$$

A longitudinal tip over criterion requires that the line between the main gear and the CG be at least 15° relative to the vertical such that the aircraft will not tip back on its tail at a maximum nose-up attitude [16]. This puts a lower bound on the x-location of the main gear. Note that $\tan(\phi)$ is a design variable here, instead of ϕ , to make the constraint SP-compatible.

$$x_m \geq (l_m + z_{CG}) \tan(\phi) + x_{CG} \quad (107)$$

$$\tan(\phi) \geq \tan(\phi_{min}) \quad (108)$$

A lateral tip over constraint is introduced to ensure that an aircraft does not tip over in a turn [23]. The turnover angle is defined as

$$\tan \psi = \frac{z_{CG_0} + l_m}{\Delta x_n \sin \delta} \quad (109)$$

where

$$\tan \delta = \frac{y_m}{B}. \quad (110)$$

Using the relationship

$$\cos\left(\arctan\left(\frac{y_m}{B}\right)\right) = \frac{B}{\sqrt{B^2 + y_m^2}}, \quad (111)$$

this constraint can, perhaps surprisingly, be rewritten in, not only SP-compatible, but GP-compatible form as

$$1 \geq \frac{(z_{CG_0} + l_m)^2 (y_m^2 + B^2)}{(\Delta x_n y_m \tan(\psi))^2} \quad (112)$$

Typically this angle, ψ , should be no larger than 63° [16].

$$\tan(\psi) \leq \tan(\psi_{max}) \quad (113)$$

The aircraft must be able to rotate on its main wheels at takeoff without striking the tail of the fuselage and, similarly, must be able to land on its main gear without striking the tail [16]. This constrains the location of the main gear. More specifically, the horizontal distance between the main gear and the point at which the fuselage sweeps up towards the tail must be sufficiently small, relative to the length of the main gear, such that the angle relative to the horizontal from the main wheels to the upsweep point is greater than the takeoff/landing angles. The result is a signomial constraint that imposes a lower bound on the length of the gear and the x-location of the main gear.

$$\frac{l_m}{\tan(\theta_{TO})} \geq x_{up} - x_m \quad (114)$$

The length of the main gear is also constrained by the engine diameter, because the engines must have sufficient clearance from the ground. A signomial constraint provides another lower bound on the length of the main gear.

$$l_m + (y_{eng} - y_m) \tan(\gamma) \geq d_{nacelle} + h_{nacelle} \quad (115)$$

The landing gear position in the spanwise (y) direction is, on one side, lower bounded by the length of the gear itself and, on the other side, upper bounded by the spanwise location of the engines. Both of these constraints are necessary to allow the landing gear to retract in the conventional manner for typical narrowbody commercial aircraft.

$$y_m \geq l_m \quad (116)$$

$$y_m \leq y_{eng} \quad (117)$$

Oleo-pneumatic shock absorbers are common to landing gear for large aircraft. Their purpose is to reduce the vertical load on the aircraft at touchdown, and they are typically sized by a hard landing condition. The maximum stroke of the shock absorber can be determined by considering the aircraft's kinetic energy, and the target maximum load [24].

$$E_{land} = \frac{W_0}{2g} w^2 \quad (118)$$

$$S = \frac{1}{\eta_s} \frac{E_{land}}{L_m \lambda} \quad (119)$$

As a preliminary model, the oleo size can be estimated using historical relations that are conveniently in monomial form [16]. The length of the main gear must be greater than the length of the oleo and the radius of the tires.

$$l_{oleo} = 2.5S \quad (120)$$

$$d_{oleo} = 1.3 \sqrt{\frac{4\lambda L_M / n_{mg}}{\rho_{oleo} \pi}} \quad (121)$$

$$l_m \geq l_{oleo} + \frac{d_{tm}}{2} \quad (122)$$

The weight of each strut for both the main and nose struts is lower bounded by assuming a thin walled cylinder with constant cross sectional area.

$$W_{ms} \geq 2\pi r_m t_m l_m \rho_{st} g \quad (123)$$

$$W_{ns} \geq 2\pi r_n t_n l_n \rho_{st} g \quad (124)$$

The cross-sectional area is itself constrained by the compressive yield of the landing gear material and the maximum load exerted on each strut.

$$2\pi r_m t_m \sigma_{yc} \geq \frac{\lambda L_m N_s}{n_{mg}} \quad (125)$$

$$2\pi r_n t_n \sigma_{yc} \geq (L_n + L_{n_{dyn}}) N_s \quad (126)$$

Another, typically more restrictive, structural constraint ensures the struts will not buckle. This constrains the area moment of inertia of the strut cross section, which in turn puts upward pressure on the radius and thickness of the struts. Again, a thin walled cylinder approximation is made. The buckling constraint assumes that no side force is exerted on the cylinder, which is perhaps a weak assumption due to forces exerted in braking, for example, and due to the fact that aircraft do not typically land with the main gear struts perfectly normal to the runway surface.

$$L_m \leq \frac{\pi^2 E I_m}{K^2 l_m^2} \quad (127)$$

$$I_m = \pi r_m^3 t_m \quad (128)$$

$$L_n \leq \frac{\pi^2 E I_n}{K^2 l_n^2} \quad (129)$$

$$I_n = \pi r_n^3 t_n \quad (130)$$

A machining constraint is used to ensure that the strut walls are not too thin to be fabricated [23].

$$\frac{2r_m}{t_m} \leq 40 \quad (131)$$

$$\frac{2r_n}{t_n} \leq 40 \quad (132)$$

In addition, simple retraction space constraints are used to ensure that the struts are not too wide for the gear to fit inside the fuselage.

$$2w_{t_m} + 2r_m \leq h_{hold} \quad (133)$$

$$2w_{t_n} + 2r_n \leq 0.8 \quad (134)$$

The wheel weights and sizes can be estimated using historical relations from [16, 25], which are, again, conveniently in monomial form. The nose gear tires are assumed to be 80% of the size of the main gear tires.

$$F_{wm} = \frac{L_{w_m} d_{t_m}}{1000} \quad (135)$$

$$W_{wa,m} = 1.2 F_{w_m}^{0.609} \quad (136)$$

$$F_{wn} = \frac{L_{w_n} d_{t_n}}{1000} \quad (137)$$

$$W_{wa,n} = 1.2F_{wn}^{0.609} \quad (138)$$

$$d_{t_m} = 1.63L_{w_m}^{0.315} \quad (139)$$

$$w_{t_m} = 0.104L_{w_m}^{0.480} \quad (140)$$

$$d_{t_n} = 0.8d_{t_m} \quad (141)$$

$$w_{t_n} = 0.8w_{t_m} \quad (142)$$

$$W_{mw} = n_{wps} W_{wa,m} \quad (143)$$

$$W_{nw} = n_{wps} W_{wa,n} \quad (144)$$

Finally, the total landing gear system weight is lower bounded by accounting for the weights of each assembly. We use an additional weight fraction to account for weight that is proportional to the weight of the wheels [25].

$$W_{add_m} = 1.5W_{mw} \quad (145)$$

$$W_{add_n} = 1.5W_{nw} \quad (146)$$

$$W_{mg} \geq n_{mg} (W_{ms} + W_{mw} + W_{add_m}) \quad (147)$$

$$W_{ng} \geq W_{ns} + W_{nw} + W_{add_n} \quad (148)$$

$$W_{lg} \geq W_{mg} + W_{ng} \quad (149)$$

3. Model Results

Using fixed values representative of the benchmark aircraft, a solution was obtained for this **SP**. Tables of the optimal values and the constant values used can be found in the appendix. Solving the **SP** took 5 **GP** solves and 0.388 seconds. Although some of the solution values show good agreement with the values for the benchmark aircraft, other values, for example the total landing gear weight, show poorer agreement. This is likely due to the relatively low fidelity weight model used for this work.

Table 9: Solution comparison with the benchmark aircraft

Free Variable	Value	Estimate for benchmark aircraft
B [m]	16.3	15.6 [14]
T [m]	5.59	5.72 [14]
W_{lg} [kg]	1500	4000 [5]

The objective function value is most sensitive to the fuselage upsweep point: a 1% increase in the fuselage upsweep x-coordinate would result in a 1.4% increase in the weight of the landing gear, according to the model. Unsurprisingly, the objective function is also sensitive to the weight of the aircraft: a 1% decrease in the aircraft weight would result in a 0.98% reduction in the landing gear weight. Finally, this model predicts that landing gear weight is also sensitive to the x-location of the **CG**. If the **CG** moves towards the tail an extra 1%, the landing gear weight is expected to decrease by 0.96%.

V. Conclusion

In this work, signomial programming has been used to tackle aircraft design problems. More specifically, signomial programming models have been created to find the optimal preliminary sizing of a commercial tube-and-wing aircraft's vertical tail, fuselage, and landing gear. In doing so, signomial programming has been demonstrated as a viable approach to multidisciplinary aircraft design optimization, with a wide range of constraints fitting naturally into the required formulation. The models are readily extensible and easily combined with other models, making them good building blocks for a full aircraft model. Though not as rigorous as for geometric programs, the solution method for signomial programs is disciplined and effective. A significant improvement in fidelity over previous geometric programming models has been achieved thanks to the relaxed restrictions on signomial programs. Lagrange multipliers obtained from the solution procedure mean that, in addition to finding an optimal design, the models also give local sensitivities to fixed variables, thus giving insight into the design space.

Appendix: Model Results

A. Vertical Tail Model

Table 10: Vertical tail model design variable solution values and constant values

Free Variables	Value	Units	Constants	Value	Units
Vertical Tail			Vertical Tail		
A_{vt}	1.81	[-]	A_{eng}	2.405	[m ²]
$C_{D_{vis}}$	0.005164	[-]	$C_{D_{wm}}$	0.5	[-]
$C_{L_{vt}}$	0.4505	[-]	$C_{L_{wmax}}$	2.6	[-]
D_{vis}	1698	[N]	L_{fuse}	39	[m]
D_{wm}	3112	[N]	T_e	1.29e+05	[N]
L_{max}	1.043e+06	[N]	V_1	65	[m/s]
L_{vt}	3.683e+04	[N]	V_c	234	[m/s]
Re_c	2.946e+07	[-]	V_{ne}	144	[m/s]
S	63.19	[m ²]	μ	1.4e-05	[N * s/m ²]
S_{vt}	31.6	[m ²]	ρ_c	0.38	[kg/m ³]
W_{struct}	2662	[N]	ρ_{TO}	1.225	[kg/m ³]
W_{vt}	1331	[N]	$\tan(\Lambda_{LE})$	0.8391	[-]
Δx_{lead}	14.42	[m]	$c_{l_{vt}}$	0.5	[-]
Δx_{trail}	21	[m]	e	0.8	[-]
λ	0.27	[-]	l_e	4.83	[m]
τ	0.15	[-]	x_{CG}	18	[m]
b	15.12	[m]	Vertical Tail Structure		
b_{vt}	7.562	[m]	N_{lift}	2	[-]
\bar{c}	4.638	[m]	ρ_{cap}	2700	[kg/m ³]
c_{root}	6.58	[m]	ρ_{web}	2700	[kg/m ³]
c_{tip}	1.776	[m]	$\sigma_{max, shear}$	1.67e+08	[Pa]
l_{vt}	17.32	[m]	σ_{max}	2.5e+08	[Pa]
p	1.54	[-]	$f_{w, add}$	0.4	[-]
q	1.27	[-]	g	9.81	[m/s ²]
$z_{\bar{c}}$	2.079	[m]	r_h	0.75	[-]
Vertical Tail Structure			w	0.5	[-]
A	3.62	[-]			
I_{cap}	3.359e-06	[-]			
L_{max}	1.043e+06	[N]			
M_r	2.424e+05	[N]			
S	63.19	[m ²]			
W_{cap}	5535	[N]			
W_{struct}	2662	[N]			
W_{web}	1120	[N]			
λ	0.27	[-]			
ν	0.8327	[-]			
τ	0.15	[-]			
b	15.12	[m]			
p	1.54	[-]			
q	1.27	[-]			
I_{cap}	0.0007129	[-]			
I_{web}	0.0006414	[-]			

B. Fuselage Model

Table 11: Fuselage model design variable solution values and constant values

Free Variables	Value	Units	Constants	Value	Units
A_{floor}	0.01569	$[m^2]$	LF	0.898	$[-]$
A_{fuse}	10.81	$[m^2]$	L_{vmax}	3.5e+04	$[N]$
A_{hold}	1.026	$[m^2]$	N_{land}	6	$[-]$
A_{skin}	0.01087	$[m^2]$	R	287	$[J/K/kg]$
D	1.35e+04	$[N]$	S_{PR}	6	$[-]$
$D_{friction}$	7988	$[N]$	T_{cabin}	300	$[K]$
$D_{upsweep}$	5513	$[N]$	V_{∞}	234	$[m/s]$
FF	1.076	$[-]$	W''_{floor}	60	$[N/m^2]$
M_{floor}	4.442e+05	$[N * m]$	W''_{insul}	22	$[N/m^2]$
P_{floor}	1.137e+06	$[N]$	W_{seat}	150	$[N]$
Q_v	1.005e+05	$[N * m]$	W''_{window}	435	$[N/m]$
R_{fuse}	1.855	$[m]$	$W_{avg.pass}$	180	$[lbf]$
S_{bulk}	21.62	$[m^2]$	W_{cargo}	1e+04	$[N]$
S_{floor}	5.686e+05	$[N]$	$W_{carryon}$	15	$[lbf]$
S_{nose}	49.82	$[m^2]$	$W_{checked}$	40	$[lbf]$
V_{bulk}	0.02016	$[m^3]$	W_{fix}	3000	$[lbf]$
V_{cabin}	315	$[m^3]$	Δh	1	$[m]$
V_{cargo}	6.796	$[m^3]$	Δp	5.2e+04	$[Pa]$
V_{cone}	0.007483	$[m^3]$	μ	1.4e-05	$[N * s/m^2]$
V_{cyl}	0.2653	$[m^3]$	ρ_{∞}	0.38	$[kg/m^3]$
V_{floor}	0.04902	$[m^3]$	ρ_{bend}	2700	$[kg/m^3]$
V_{hold}	25.04	$[m^3]$	ρ_{cargo}	150	$[kg/m^3]$
$V_{luggage}$	18.24	$[m^3]$	ρ_{cone}	2700	$[kg/m^3]$
V_{nose}	0.04645	$[m^3]$	ρ_{floor}	2700	$[kg/m^3]$
W_{apu}	5657	$[N]$	$\rho_{luggage}$	100	$[kg/m^3]$
W_{buoy}	1517	$[N]$	ρ_{skin}	2700	$[kg/m^3]$
W_{cone}	356.7	$[N]$	σ_{floor}	2.069e+08	$[N/m^2]$
W_{floor}	6570	$[N]$	σ_{skin}	1.034e+08	$[N/m^2]$
W_{fuse}	1.507e+05	$[N]$	τ_{floor}	2.069e+08	$[N/m^2]$
W_{insul}	4307	$[N]$	b_v	7	$[m]$
$W_{luggage}$	1.79e+04	$[N]$	c_{vt}	4	$[m]$
W_{padd}	6.465e+04	$[N]$	f_{apu}	0.035	$[-]$
W_{pass}	1.337e+05	$[N]$	f_{fadd}	0.2	$[-]$
W_{pay}	1.616e+05	$[N]$	f_{frame}	0.25	$[-]$
W_{seat}	2.79e+04	$[N]$	$f_{lugg.1}$	0.4	$[-]$
W_{shell}	1.582e+04	$[N]$	$f_{lugg.2}$	0.1	$[-]$
W_{skin}	8791	$[N]$	f_{padd}	0.4	$[-]$
W_{window}	1.062e+04	$[N]$	f_{string}	0.35	$[-]$
λ_{cone}	0.4	$[-]$	g	9.81	$[m/s^2]$
ϕ	0.1749	$[-]$	n_{seat}	186	$[-]$
ρ_{cabin}	0.8711	$[kg/m^3]$	p_{cabin}	7.5e+04	$[Pa]$
σ_x	3.831e+07	$[N/m^2]$	p_s	31	$[in]$
σ_{θ}	1.034e+08	$[N/m^2]$	r_E	1	$[-]$
τ_{cone}	1.034e+08	$[N/m^2]$	w_{aisle}	0.51	$[m]$
f	10.68	$[-]$	w_{seat}	0.5	$[m]$
h_{floor}	0.3712	$[m]$	w_{sys}	0.1	$[m]$
h_{hold}	0.4838	$[m]$			
l_{cone}	10	$[m]$			
l_{floor}	28.12	$[m]$			
l_{fuse}	39.61	$[m]$			
l_{nose}	5.2	$[m]$			
l_{shell}	24.41	$[m]$			
n_{pass}	167	$[-]$			
n_{rows}	31	$[-]$			
p_{λ_v}	1.6	$[-]$			
q_{λ_v}	1.3	$[-]$			
t_{cone}	4.494e-05	$[m]$			
t_{shell}	0.001259	$[m]$			
t_{skin}	0.0009324	$[m]$			
w_{floor}	3.125	$[m]$			
x_{shell}	5.2	$[m]$			

C. Landing Gear Model

Table 12: Landing gear model design variable solution values and constant values

Free Variables	Value	Units	Constants	Value	Units
B	16.29	[m]	E	205	[GPa]
E_{land}	3.809e+05	[J]	K	2	[-]
F_{w_m}	7159	[-]	N_s	2	[-]
F_{w_n}	643.7	[-]	W_0	8.044e+05	[N]
I_m	7.545e-06	[m ⁴]	η_s	0.8	[-]
I_n	8.916e-07	[m ⁴]	λ	2.5	[-]
L_m	6.435e+05	[N]	ρ_{st}	7850	[kg/m ³]
L_n	1.609e+05	[N]	σ_{yc}	4.7e+08	[Pa]
$L_{n_{dyn}}$	6.617e+04	[N]	$\tan(\gamma)$	0.08749	[-]
L_{w_m}	1.609e+05	[N]	$\tan(\phi_{min})$	0.2679	[-]
L_{w_n}	8.044e+04	[N]	$\tan(\psi_{max})$	1.963	[-]
S	0.2959	[m]	$\tan(\theta_{TO})$	0.2679	[-]
T	5.585	[m]	$d_{nacelle}$	2	[m]
W_{add_m}	3565	[N]	g	9.81	[m/s ²]
W_{add_n}	822.2	[N]	h_{hold}	1	[m]
W_{lg}	1.46e+04	[N]	$h_{nacelle}$	0.5	[m]
W_{mg}	1.311e+04	[N]	n_{mg}	2	[-]
W_{ms}	612	[N]	n_{wps}	2	[-]
W_{mw}	2377	[N]	p_{oleo}	1800	[psi]
W_{ng}	1488	[N]	w	10	[ft/s]
W_{ns}	117.4	[N]	x_{CG_0}	18	[m]
W_{nw}	548.1	[N]	x_{up}	28	[m]
$W_{wa,m}$	267.2	[lbf]	y_{eng}	4.83	[m]
$W_{wa,n}$	61.61	[lbf]	z_{CG}	2	[m]
Δx_m	3.257	[m]	z_{wing}	0.5	[m]
Δx_n	13.03	[m]			
$\tan(\phi)$	0.2679	[-]			
$\tan(\psi)$	1.963	[-]			
d_{oleo}	0.3735	[m]			
d_{t_m}	1.179	[m]			
d_{t_n}	0.9041	[m]			
l_m	2.322	[m]			
l_n	1.577	[m]			
l_{oleo}	0.7399	[m]			
r_m	0.06639	[m]			
r_n	0.04296	[m]			
t_m	0.008205	[m]			
t_n	0.00358	[m]			
w_{t_m}	0.4088	[m]			
w_{t_n}	0.327	[m]			
x_m	21.29	[m]			
x_n	5	[m]			
x_{CG}	18.03	[m]			
y_m	2.793	[m]			

Acknowledgments

This work is partially-funded by the NASA Aeronautics Graduate Fellowship.

References

- [1] Hoburg, W. and Abbeel, P., “Geometric programming for aircraft design optimization,” *AIAA Journal*, Vol. 52, No. 11, 2014, pp. 2414–2426.
- [2] Boyd, S., Kim, S.-J., Vandenberghe, L., and Hassibi, A., “A tutorial on geometric programming,” *Optimization and engineering*, Vol. 8, No. 1, 2007, pp. 67–127.
- [3] Kroo, I., Altus, S., Braun, R., Gage, P., and Sobieski, I., “Multidisciplinary optimization methods for aircraft preliminary design,” *AIAA paper*, Vol. 4325, 1994, pp. 1994.
- [4] Henderson, R. P., Martins, J., and Perez, R. E., “Aircraft conceptual design for optimal environmental performance,” *Aeronautical Journal*, Vol. 116, No. 1175, 2012, pp. 1.
- [5] Drela, M., “TASOPT 2.08 Transport Aircraft System OPTimization,” *MIT*, 2011.
- [6] de Weck, O., Agte, J., Sobieski, J., Arendsen, P., Morris, A., and Spieck, M., “State-of-the-art and future trends in multidisciplinary design optimization,” *Proceedings of the 48th AIAA/ASME/ASCE/AHS/ASC Structures, Structural Dynamics, and Materials Conference*, AIAA, Vol. 1905, 2007.
- [7] Martins, J. R. and Lambe, A. B., “Multidisciplinary design optimization: a survey of architectures,” *AIAA journal*, Vol. 51, No. 9, 2013, pp. 2049–2075.
- [8] Duffin, R. J., Peterson, E. L., and Zener, C., *Geometric programming: theory and application*, Wiley New York, 1967.
- [9] Mehrotra, S., “On the implementation of a primal-dual interior point method,” *SIAM Journal on optimization*, Vol. 2, No. 4, 1992, pp. 575–601.
- [10] Hoburg, W. and Abbeel, P., “Fitting Geometric Programming Models to Data,” 2014.
- [11] Boyd, S., “Sequential convex programming,” *Lecture Notes*, Stanford University, 2008.
- [12] Burnell, E. and Hoburg, W., “Gpkit,” <https://github.com/convexopt/gpkit>, 2015, Version 0.3.4.
- [13] ApS, M., *The MOSEK C optimizer API manual. Version 7.1 (Revision 41)*, 2015.
- [14] Boeing Commercial Airplanes, “737 MAX Airplane characteristics for airport planning,” *Seattle, Washington, USA*, 2015.
- [15] Brady, C., “The Boeing 737 Technical Site,” <http://www.b737.org.uk>, 2015 (accessed November 1st 2015).
- [16] Raymer, D. P., “Aircraft Design: A Conceptual Approach . Washington DC: American Institute of Aeronautics and Astronautics,” 1992.
- [17] Boeing, “737 Airplane characteristics for airport planning,” *Seattle, Washington, USA*, 2007.
- [18] Anderson, J. D., “Fundamentals of aerodynamics, 2001,” .
- [19] Kroo, I. and Shevell, R., “Aircraft design: Synthesis and analysis,” *Desktop Aeronautics Inc., Textbook Version 0.99*, 2001.
- [20] Hoburg, W., Kirschen, P., and Abbeel, P., “Fitting Geometric Programming Models to Data,” *Optimization and Engineering*.
- [21] Drela, M., “XFOIL: An analysis and design system for low Reynolds number airfoils,” *Low Reynolds number aerodynamics*, Springer, 1989, pp. 1–12.
- [22] Harris, J. W. and Stöcker, H., *Handbook of mathematics and computational science*, Springer Science & Business Media, 1998.
- [23] Chai, S. T. and Mason, W. H., *Landing gear integration in aircraft conceptual design*, Master’s thesis, Virginia Polytechnic Institute and State University, 1996.
- [24] Torenbeek, E., *Synthesis of subsonic aircraft design*, 1982.
- [25] Currey, N. S., *Landing Gear Design Handbook*, Lockheed-Georgia Company, 1984.